

## ARTICLE

# Usefulness of contrast-enhanced magnetic resonance imaging for evaluating solitary pulmonary nodules

Kiminori Fujimoto

*Department of Radiology, Kurume University School of Medicine and Center for Diagnostic Imaging,  
Kurume University Hospital, 67 Asahi-machi, Kurume, Fukuoka, 830-0011 Japan*

*Corresponding address: Dr Kiminori Fujimoto, MD, PhD, Associate Professor and Head of Diagnostic Thoracic Imaging,  
Department of Radiology, Kurume University School of Medicine and Center for Diagnostic Imaging,  
Kurume University Hospital, 67 Asahi-machi, Kurume, Fukuoka, 830-0011 Japan.*

*Email: kimichan@med.kurume-u.ac.jp*

Date accepted for publication 30 October 2007

### Abstract

Evaluation of solitary pulmonary nodules (SPNs) poses a challenge to radiologists. Chest computed tomography (CT) is considered the standard technique for assessing morphologic findings and intrathoracic spread of an SPN. Although the clinical role of magnetic resonance imaging (MRI) for SPNs remains limited, considerable experience has been gained with MRI of thoracic diseases. Dynamic MRI and dynamic CT are useful for differentiating between malignant and benign SPNs (especially tuberculomas and hamartomas). Furthermore, dynamic MRI is useful for assessing tumor vascularity, interstitium, and vascular endothelial growth factor expression, and for predicting survival outcome among patients with peripheral pulmonary carcinoma. These advantages make dynamic MRI a promising method and a potential biomarker for characterizing tumor response to anti-angiogenic treatment as well as for predicting survival outcomes after treatment.

**Keywords:** *Solitary pulmonary nodule; magnetic resonance imaging; contrast enhancement; lung cancer; angiogenesis.*

### Introduction

A solitary pulmonary nodule (SPN) is defined as an approximately round lesion less than 3 cm in diameter that is completely surrounded by pulmonary parenchyma without other pulmonary abnormalities<sup>[1]</sup>. A lesion larger than 3 cm is more appropriately termed a pulmonary “mass”<sup>[2]</sup> and is not included in the definition of SPN because many of these lesions are malignant<sup>[3]</sup>. An SPN is found on 0.09% to 0.20% of all chest radiographs, and an estimated 150 000 such nodules are identified each year in the United States<sup>[1]</sup>. Recent advanced technology, such as low-dose, helical computed tomography (CT) screening and multi-detector row CT, has increased the incidental detection rate of SPNs.

Once an SPN is detected, imaging techniques can be used to characterize the nodule in terms of whether it is likely to be benign or malignant<sup>[4]</sup>. Absence of growth

over a 2-year period is highly suggestive of a benign lesion, but many patients do not have comparative chest radiographs. Non-surgical tests to help distinguish benign from malignant nodules include various CT techniques<sup>[1–10]</sup>, transbronchoscopic biopsy, transthoracic fine-needle aspiration biopsy<sup>[11]</sup>, and, more recently, 2-[<sup>18</sup>F]fluoro-2-deoxy-D-glucose (FDG)-positron emission tomography (PET)<sup>[12–14]</sup> and dynamic contrast-enhanced magnetic resonance imaging (MRI)<sup>[15–21]</sup>. Chest CT is considered the standard technique for assessing morphologic findings<sup>[1–5]</sup> and intrathoracic spread of an SPN. Various strategies other than morphologic evaluations are also applied to the differentiation of malignant and benign nodules, including growth rate assessment<sup>[6]</sup>, Bayesian analysis<sup>[7]</sup>, and the hemodynamic characteristics of dynamic helical CT<sup>[8–10]</sup>.

Based on the suggestions for work-up of pulmonary nodules by the Fleischner Society<sup>[5]</sup> and as described

by Winer-Muram<sup>[3]</sup>, in small nodules ( $\leq 10$  mm maximum diameter, 8 mm average length and width) the work-up is usually based on non-invasive techniques which include: (a) short-term follow-up with unenhanced CT demonstrates spontaneous decrease in size confirming a benign nodule; (b) follow-up with unenhanced low-dose CT for up to 2 years excludes growth, again confirming a benign lesion; (c) FDG-PET with CT follow-up is chosen if no glucose uptake is demonstrated, but biopsy is necessary if glucose uptake is shown; and (d) contrast-enhanced CT or MRI with CT follow-up is chosen if no significant enhancement is shown, but biopsy is necessary if significant enhancement is shown. In larger nodules ( $>10$  mm) immediate biopsy should be considered. Biopsy specimens obtained by transbronchoscopic biopsy of an SPN often fail to lead to a pathologic diagnosis. Although transthoracic needle aspiration biopsy has better sensitivity, there is a risk of pneumothorax and hemorrhage<sup>[11]</sup>, as well as a false negative result, which may lead to an unacceptable therapeutic delay in early-stage lung cancer. In the end, a surgical procedure is often required to establish the final diagnosis.

There are some problematic issues in evaluating the contrast-enhancement or glucose-uptake of an SPN. An SPN in which the increase in attenuation with contrast-material is less than 15 Hounsfield units (HU) is likely to be benign<sup>[8]</sup>, but with an increase in attenuation of more than 15 HU, there is a wide overlap between benign and malignant SPNs. One dynamic CT study showed high sensitivity and negative predictive values for the diagnosis of malignant nodules, but low specificity because of the presence of highly enhancing benign nodules<sup>[9]</sup>. In a recent meta-analysis assessing nodular metabolic characteristics on FDG-PET to characterize SPNs, the sensitivity for detecting malignancy was 97%, with a specificity of 78%<sup>[12]</sup>. Thus, the sensitivity of FDG-PET for characterizing nodules is sufficiently high for use in clinical patient management. Unfortunately, the accuracy seems to decrease for small nodules, particularly in cases of non-solid lesions. One report suggested that pulmonary nodules that are less than 1 cm in size or show faint images, including ground-glass opacity on CT, cannot be evaluated accurately by FDG-PET<sup>[13]</sup>. FDG is not a tumor-specific tracer and is also taken up in benign diseases. Furthermore, increased FDG uptake is also observed in inflammatory cells<sup>[14]</sup>.

MRI has some shortcomings in thoracic imaging, such as: (a) low signal-to-noise ratio due to low proton density in inflated lungs; (b) susceptibility artifacts caused by many air-tissue interfaces; and (c) motion artifact vulnerability related to a relatively long acquisition time and intrinsic cardiac pulsation and respiration<sup>[22]</sup>. On the other hand, MRI provides high-contrast definition of normal and abnormal tissues. Furthermore, intrinsic flow sensitivity and the absence of ionizing radiation are advantages of MRI over CT. Although there is a

limitation to the frequency of obtaining the same plane images on CT because of X-ray exposure, dynamic MRI allows for repeated same-plane images.

MRI has a potential role in the accurate staging of non-small-cell lung cancer, such as evaluation of tumor invasion through the superior sulcus<sup>[23]</sup>, detection of mediastinal invasion<sup>[24]</sup>, and prediction of hilar and mediastinal nodal metastasis<sup>[25]</sup>. The results of several studies in which MRI was used to assess pulmonary lesions suggest that the kinetics indexes and morphologic parameters of dynamic MRI are helpful in differentiating between malignant and benign lesions; the problem of differentiating between benign inflammatory and malignant lesions remains, although MRI and CT can relatively reliably differentiate between benign hamartomas and granulomas and malignant lesions<sup>[15–20]</sup>. Moreover, dynamic MRI has been investigated for a range of clinical oncologic applications, including cancer detection, diagnosis, staging, and assessment of treatment response<sup>[21]</sup>. Tumor microvascular measurements by dynamic MRI correlate with prognostic factors (such as microvessel density and vascular endothelial growth factor expression) and with recurrence and survival outcomes<sup>[16,21]</sup>.

In this paper, the clinical role of dynamic contrast-enhanced MRI for evaluating SPNs, e.g. to differentiate between benign and malignant SPNs and imaging-pathology correlation, is illustrated and reviewed.

## Imaging techniques for contrast-enhanced dynamic MRI

We previously reported on the use of dynamic MR scans obtained with T1-weighted spin-echo sequences (repetition time, 120–150 ms; echo time, 10 ms) and oblique sagittal or transverse images, all during breathhold (approximately 15–16 s)<sup>[15,16]</sup>. After the first spin-echo sequence, gadopentetate dimeglumine was administered and contrast-enhanced dynamic MR images were obtained from 1 to 8 min after the injection (Fig. 1A). Although this technique is comparatively traditional, it has been used for many dynamic MRI studies for assessing the kinetic and quantitative signal intensity changes of various neoplasms in various organs before evaluation with the fast scan sequences.

Two major techniques were developed recently, which appear to be more suitable for enhanced dynamic MRI with gadolinium containing contrast materials: the fast (or turbo) spin-echo sequence and fast gradient-echo sequence<sup>[17–20]</sup>. The fast spin-echo sequence is proposed to reduce susceptibility artifacts and to increase the signal-to-noise ratio. This sequence is a multi-echo spin-echo sequence where different parts of k-space are recorded by different spin echoes and this sequence is based on rapid repetitive rephasing with a train of multiple  $180^\circ$  refocusing pulses, particularly with short echo spacing. In contrast, in a gradient-echo sequence, a gradient is used instead of a  $180^\circ$  radio-frequency pulse

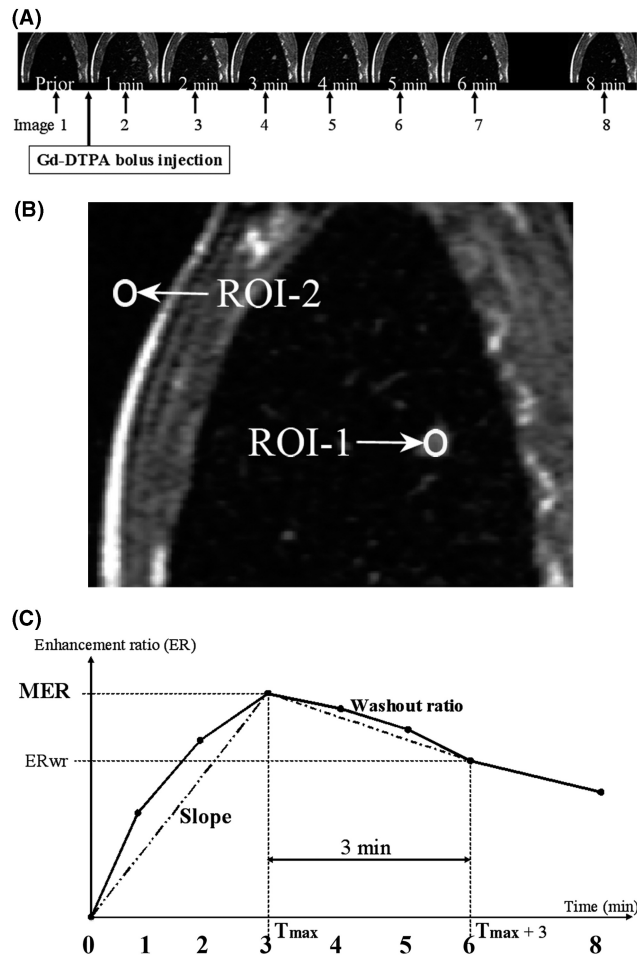


**Figure 1** (A) Dynamic MRI enhancement protocol. After the first spin-echo sequence, a bolus of 0.1 mmol of gadopentetate dimeglumine (Gd-DTPA) per kilogram of body weight was injected intravenously for 10 s. A total of eight sagittal-oblique dynamic MR images (referential case) were obtained in a 65-year-old man with adenocarcinoma. (B) The image was obtained 1 min after Gd-DTPA injection. Note the placement of the region-of-interest (ROI). ROI-1 and ROI-2 indicate areas of the pulmonary nodule and background noise, respectively. (C) The time–enhancement ratio curve obtained by calculating signal intensities of ROIs (see description). MER, maximum enhancement ratio (%);  $T_{max}$ , time at MER (min); ERwr, enhancement ratio at  $T_{max} + 3$  min (%); Slope, slope value of the time–enhancement ratio curve,  $MER/T_{max}$  (%/min); Washout ratio =  $([MER - ERwr]/MER) \times 100$  (%/min).

to rephase the spins. Imaging with a gradient echo is intrinsically more sensitive to magnetic field inhomogeneities because of the use of the refocusing gradient. The use of a small flip angle and a gradient for refocusing the magnetization vectors gives this sequence a time advantage. Therefore, it is widely used for fast scan images, including three-dimensional acquisitions. As the three-dimensional fast gradient echo pulse sequence is used for the shortest repetition time and echo time, it involves the use of one of the fastest sequences currently available and can be used to analyze volumetric data.

### Imaging data analysis

Signal enhancement observed on dynamic acquisition of T1-weighted images can be assessed either by analyzing

signal intensity changes and/or by quantifying contrast agent concentration changes using pharmacokinetic modeling techniques<sup>[15–20,26]</sup>. Quantitative methods use pharmacokinetic modeling techniques applied to tissue contrast agent concentration changes. Signal intensity changes during dynamic acquisition are used to estimate contrast agent concentration in vivo<sup>[27]</sup>.

The pharmacokinetic modeling techniques used in our studies<sup>[15,16,20]</sup> are similar to those used in other studies<sup>[17–19]</sup>. Assessing the coordinate plane for the time–enhancement ratio curve may be created by plotting the time ( $x$ -axis) against the percent change in signal intensity ( $y$ -axis). In our studies<sup>[15,16,20]</sup>, the time–enhancement ratio curves were obtained by calculating the percentage increase in signal intensity at any given time compared with the signal intensity before injection

of contrast material and plotting this percent increase in signal intensity against time (Fig. 1). Images were analyzed for maximum enhancement ratio, time at maximum enhancement ratio, slope of time enhancement ratio curves, and washout ratio<sup>[16,20]</sup>. In addition, the time–enhancement ratio curves were classified into three major types as follows: type A had an early peak; type B had a late peak; and type C had a gradually increasing pattern without a peak.

### Correlation with pathologic findings of the tumor and prognosis

The degree of signal enhancement on T1-weighted MRI is dependent on a number of physiological and physical factors. These include tissue perfusion, capillary permeability to the contrast agent, extracellular leakage space volume, native T1-relaxation rates of the tissue, contrast agent dose (and its protein binding), imaging sequence used, imaging parameters utilized, and machine-related factors<sup>[26]</sup>.

Many studies have attempted to correlate the contrast enhancement of various tissues with immuno-histochemical microvessel density measurements<sup>[21]</sup>. For lung cancers, some CT and MRI studies have shown broad correlations between kinetic enhancement parameter estimates and microvessel density<sup>[9,16,19]</sup>. Recently, vascular endothelial growth factor (VEGF), which is a potent vascular permeability and angiogenic factor for stimulating endothelial locomotion and proliferation<sup>[28]</sup>, was implicated as an additional explanatory factor that determines MR signal enhancement<sup>[16,19]</sup>. Moreover, VEGF is found in various types of tumor cells, and its expression is believed to have a pivotal role in angiogenesis. Such correlations between CT or MR enhancement characteristics and VEGF-related angiogenesis are evident in patients with malignant pulmonary neoplastic nodules<sup>[29]</sup>. Histologic assessment of tumor microvessel density and expression of VEGF are important prognostic factors in non-small-cell lung cancers<sup>[16]</sup>.

We previously reported that the parameters of dynamic MRI correlated with tumor vascularity and prognosis as follows [16]:

- (1) The parameters of the first half of the time-enhancement ratio curve (maximum enhancement ratio and the slope) correlated with tumor angiogenesis (microvessel count) and those of the latter half (washout ratio) correlated with tumor interstitium (degree of elastic and collagen fibers). The results suggested that intratumoral gadopentetate dimeglumine circulation depended on the quantity and distribution of small vessels, elastic fibers, and collagen fibers.
- (2) There were significantly more microvessels in patients with VEGF-positive tumors than in patients with VEGF-negative tumors. The maximum

enhancement ratio and the slope value were higher in patients with VEGF-positive tumors than in patients with VEGF-negative tumors. Furthermore there were significantly more lymph node metastases in patients with VEGF-positive tumors than in patients with VEGF-negative tumors.

- (3) The Cox proportional hazards model showed that a VEGF-positive tumor, a higher slope value, and a finding positive for lymph node metastasis were significantly related to survival. Patients with all three prognostic factors had the highest mortality rate (83%).
- (4) The findings of dynamic MRI (enhancement parameters and curve profiles) might be helpful for assessing tumor angiogenesis (microvessel count and expression of VEGF) and tumor interstitium, and might be helpful for predicting lymph node metastasis as well as the outcome of patients with peripheral pulmonary carcinomas.

### Differentiation between benign and malignant nodules

Recent studies have shown that enhancement or glucose uptake of malignant pulmonary tumors is greater than that of benign lung nodules on contrast-enhanced CT<sup>[8–10]</sup>, FDG-PET<sup>[12–14]</sup>, and contrast-enhanced MRI<sup>[15–20]</sup>. One multicenter study of lung nodule enhancement on CT reported that malignant neoplasms were significantly more enhanced than granulomas and benign neoplasms, and with 15 HU or greater as the threshold, sensitivity for malignancy was 98% (167 of 171 malignant nodules), specificity was 58% (107 of 185 benign nodules), and accuracy was 77%<sup>[8]</sup>. The authors concluded that the absence of significant lung nodule enhancement (15 HU) at CT is strongly predictive of benignity<sup>[8]</sup>. The other finding, however, was that there was a wide overlap between benign (78 of 185 nodules) and malignant SPNs with an increase in attenuation of more than 15 HU. Furthermore, one study using dynamic CT showed high sensitivity and negative predictive values for the diagnosis of malignant nodules, but low specificity because of the presence of highly enhancing benign nodules<sup>[9]</sup>.

Although active inflammation or infectious lesions are benign, they sometimes have a faster peak and/or a higher maximum enhancement ratio than malignant neoplasms. Because they are associated with increased blood flow and vessel permeability, acute inflammatory lesions and active infections are characterized by increased accumulation of contrast materials on dynamic CT or MRI. Therefore, it is difficult to differentiate between acute inflammatory lesions and active infections and malignant neoplasms based on perfusion characteristics (Fig. 2). One study suggested that the use of curve profiles in dynamic MRI as a relative specific tool is very helpful for differentiating SPNs. The possibility of visual

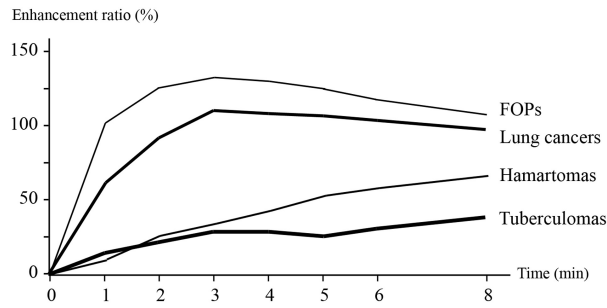


**Figure 2** Graph shows each time–enhancement curve profile of each disease group. The curves connect the medians of the enhancement ratio at each time point for each group of solitary pulmonary nodules. Note that the data are from Kono *et al.*<sup>[20]</sup>. The time–enhancement ratio curve of the focal organizing pneumonia (FOP) group shows the strongest and fastest peak of the enhancement effect; those of the hamartoma group and tuberculoma group show gradually upward profiles compared with the FOP and lung cancer groups.

estimation could simplify the evaluation; the curve profiles of dynamic MRI were found in malignant nodules having early washout and in benign lesions with a slow increase of contrast-material accumulation<sup>[19]</sup>. In this study, however, most benign lesions (11 of 16 benign nodules) were hamartomas and there were a small number of inflammatory lesions (only three non-specific inflammatory lesions and one tuberculoma). In contrast, we reported that inflammatory lesions, particularly focal organizing pneumonias, often had the dynamic curve type with an early enhancement peak and early washout (Fig. 2)<sup>[20]</sup>. The overlap of enhancement characteristics of dynamic MRI between lung cancer and focal organizing pneumonia is not surprising because malignant neoplasms and tissues with acute inflammatory lesions or infection have increased blood flow, perfusion, and capillary permeability. While focal organizing pneumonia is difficult to distinguish from lung cancer, we found that the maximum enhancement ratio and the slope value for the group of active infection and focal organizing pneumonias were higher than those for lung cancers and those for benign SPNs (tuberculomas and hamartomas) (Fig. 3)<sup>[20]</sup>. With 110% or lower maximum enhancement ratio as the cutoff value, the positive predictive value for malignancy was 92% with a sensitivity of 63% and a specificity of 74%. With 13.5%/min or greater slope value as the cutoff value, sensitivity for malignancy was 94% with a specificity of 95%, a positive predictive value of 88%, and a negative predictive value of 74%<sup>[20]</sup>. Ohno *et al.*<sup>[17]</sup> also reported that the mean relative enhancement ratio and mean slope of enhancement for the malignant SPN group were significantly higher than those for the benign SPN group and significantly lower than those for the active infection group. They concluded that

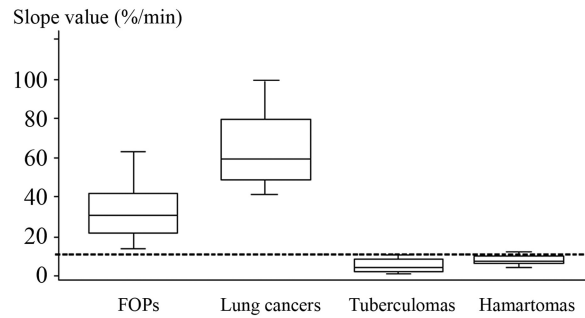


**Figure 3** Graph shows the slope values of various disease groups. Note that the data are from Kono *et al.*<sup>[20]</sup>; lung cancer group ( $n = 144$ ); FOP, focal organizing pneumonia group ( $n = 31$ ); tuberculoma group ( $n = 15$ ); and hamartoma group ( $n = 12$ ). Horizontal bars indicate medians; vertical bars, ranges. Horizontal boundaries of the boxes represent the 25th and 75th percentiles of the interquartile range. The dotted line indicates the cutoff value (13.5%/min) of the slope for differentiating lung cancer from the benign nodule group (tuberculoma and hamartoma). There is an overlap, however, between lung cancer and acute inflammatory lesions.

dynamic MR indexes were useful in the differentiation between SPNs that necessitated further evaluation or treatment (malignancy and active infection) and SPNs that did not necessitate further evaluation or treatment (benign nodules).

In summary, assessments of the maximum enhancement ratio and the slope value of dynamic MRI are helpful in differentiating benign SPNs (especially tuberculomas and hamartomas) and focal organizing pneumonias from lung cancers. The absence of significant enhancement is a strong predictor that an SPN is benign<sup>[17,20]</sup>. However, acute inflammatory lesions and active infection are often difficult to differentiate from malignant lesions based only on the perfusion characteristics (Fig. 4). A recent paper on short-term follow-up CT within 2 months<sup>[30]</sup> demonstrates that some focal lesions regress spontaneously at short term follow-up confirming the benign nature of the lesions. It is assumed that many of the lesions represent focal areas of pneumonia. Therefore, when a well-enhancing SPN with an early peak necessitating further evaluation is found, it might be useful to perform short-term follow-up CT.

### Other characteristic findings on contrast-enhanced MRI

Although dynamic study is usually not necessary, there are some useful enhancement characteristics (compared with signal intensities before and after injection of contrast material) for assessing the characteristics of an SPN.

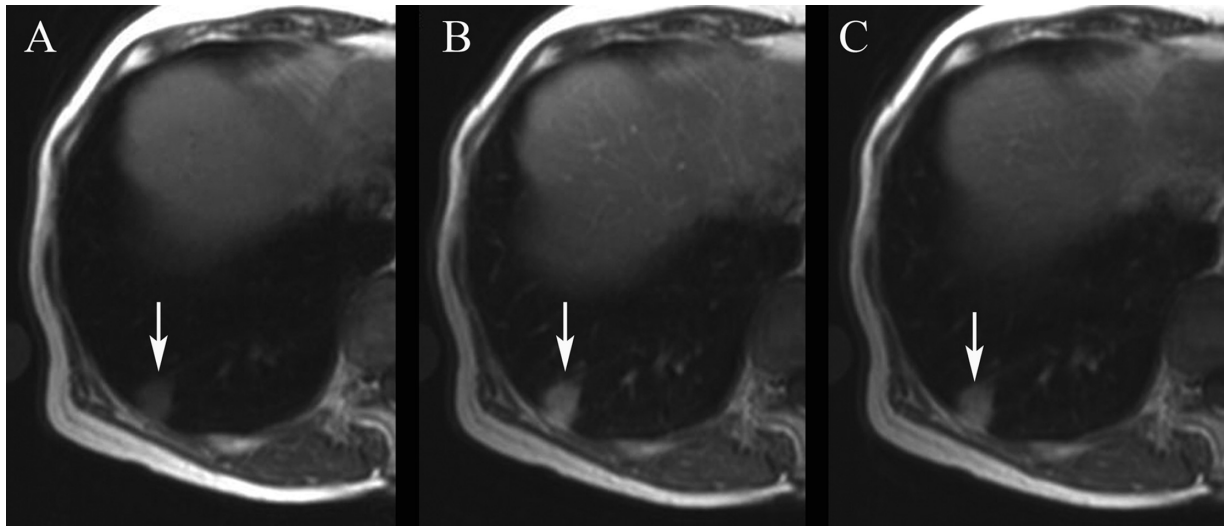


**Figure 4** A case of focal organizing pneumonia in a 52-year-old woman. The dynamic MRI scans with fast spin-echo sequence were acquired before (A) and 3 min (B) and 8 min (C) after gadopentetate dimeglumine injection. Dynamic MRI reveals a nodular lesion (arrow) showing an early and strong enhancement peak and slight washout pattern.

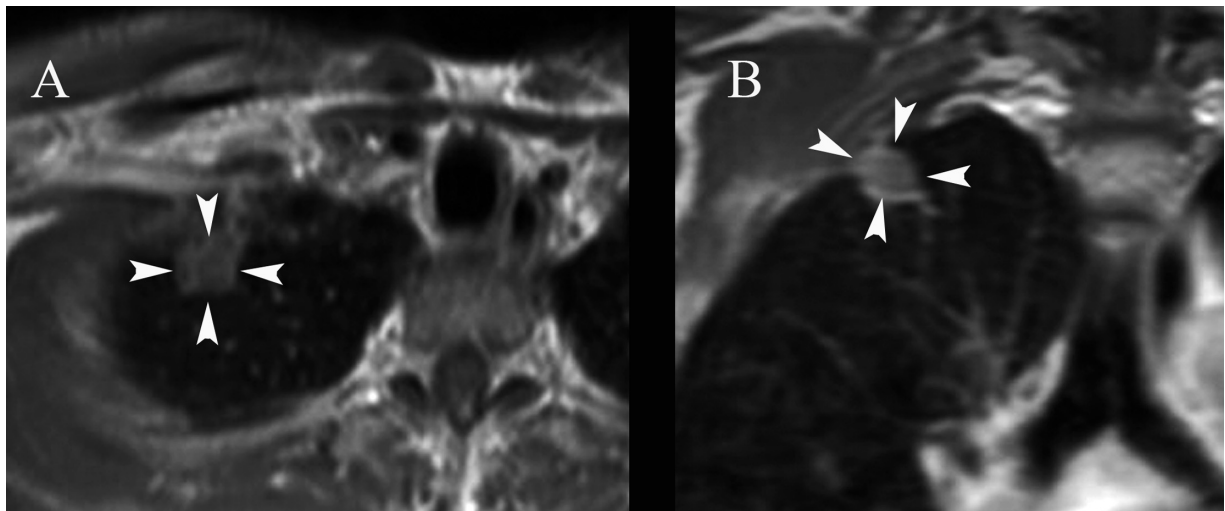


**Figure 5** A case of inactive tuberculoma in a 36-year-old man. A post-contrast-enhanced MR axial image (A) and a coronal image (B) show a nodular lesion with an area of enhancement of 2 mm or less on the outer rim of the lesion (thin-rim enhancement pattern, arrowheads).

#### *Thin-rim enhancement pattern (Fig. 5)*

Thin-rim enhancement is considered to be present when a nodular lesion has an area of enhancement limited to 2 mm or less around the outer rim of the lesion<sup>[20]</sup>. This finding is also seen on CT. The thin-rim enhancement pattern of tuberculoma on gadopentetate dimeglumine-enhanced MRI or iodinated contrast medium-enhanced CT scans was previously reported<sup>[31,32]</sup>. At histopathologic examination, the enhancing rim at the periphery of the mass corresponds to fibrous tissue surrounding epithelioid (or tuberculous) granulomas, and the area

of the central portion without contrast enhancement corresponds to caseous necrosis or scarring<sup>[20,31,32]</sup>. We found that tuberculomas had a higher prevalence of thin-rim enhancement (8 of 15 tuberculomas) than did lung cancer (0 of 144 tumors)<sup>[20]</sup>. Although thin-rim enhancement is non-specific for diagnosing tuberculoma, the finding might be suggestive of benignity<sup>[33]</sup>.

#### *Network enhancement pattern (Fig. 6)*

Network enhancement is considered to be present when enhancement of the nodular lesion is heterogeneous with areas of irregular linear enhancement and areas of

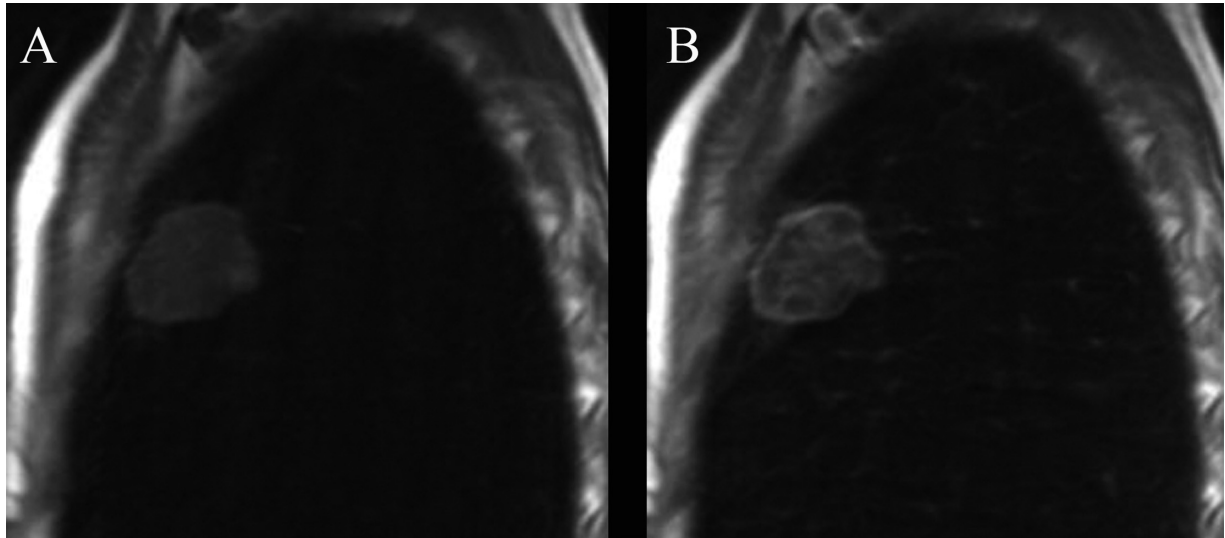


**Figure 6** A case of chondromatous hamartoma in a 58-year-old woman. The MR scans were acquired before (A) and 6 min (B) after gadopentetate dimeglumine injection. A contrast-enhanced, oblique-sagittal image shows that enhancement of the nodular lesion is heterogeneous with areas of irregular linear enhancement and areas of no enhancement (network pattern enhancement).

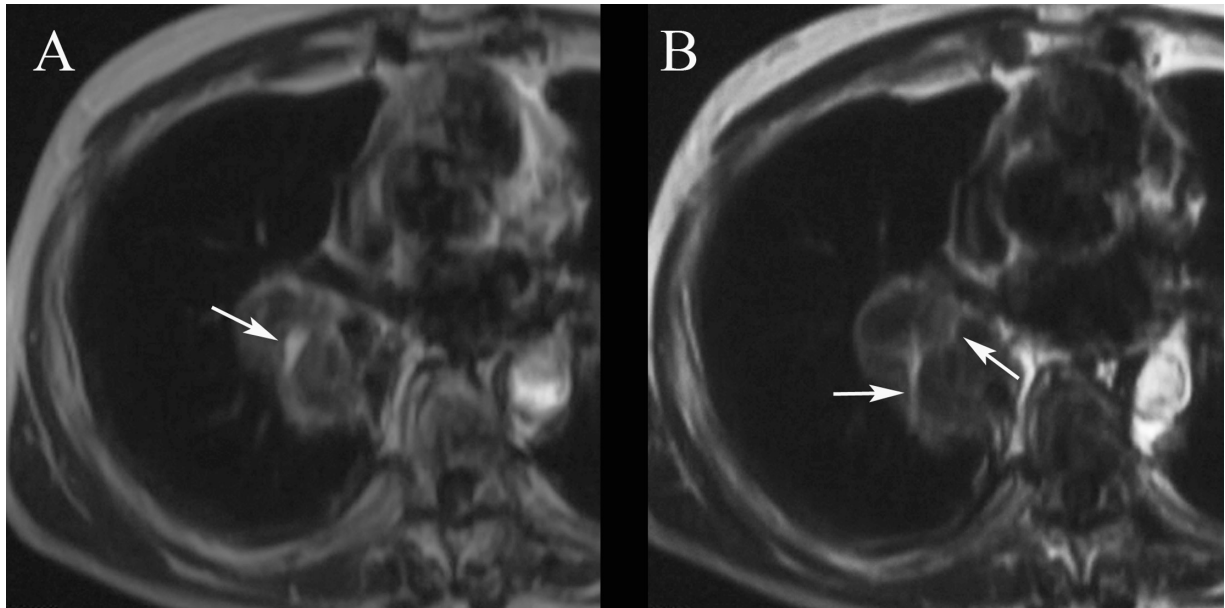


**Figure 7** A case of bronchioloalveolar adenocarcinoma in a 68-year-old man. Post contrast-enhanced T1-weighted images at the level of the aortic valve (A) and 1 cm below (B) show enhancing branching structures (pulmonary vessels, arrows) coursing through a hypo-enhanced consolidated mass. The pathologic specimens (not shown) revealed a hypo-enhancing mass containing mucinous fluid.

no enhancement<sup>[20]</sup>. Areas with no enhancement correspond to core cartilaginous tissue and septa, and areas with irregular linear enhancement correspond to cleft-like branching mesenchymal connective tissue dipping into the cartilaginous core<sup>[20,34]</sup>. Hamartomas had a higher prevalence of network enhancement (6 of 12 hamartomas) compared with the heterogeneous enhancement pattern of other SPNs (none of the other SPNs had

network enhancement)<sup>[20]</sup>. Moreover, a network enhancement pattern might not be observed in any of the malignant pulmonary nodules.

#### *Angiogram sign (Fig. 7)*

The CT angiogram sign was initially described as a specific sign of lobar bronchioloalveolar carcinoma.

It consists of normally enhancing branching pulmonary vessels in a homogeneous low-attenuating consolidation of lung parenchyma relative to the chest wall musculature, which can be caused by the production of mucin within the air spaces<sup>[35]</sup>. Recently, the CT angiogram sign was reported in both benign and malignant entities, including bronchioloalveolar carcinoma, pneumonia, pulmonary edema, obstructive pneumonitis due to central lung tumors, lymphoma, and metastasis from gastrointestinal carcinomas<sup>[36]</sup>. Although the angiogram sign is not specific for bronchioloalveolar carcinoma, it may still be considered a useful sign in imaging, including MRI. The sign is observed with a limited number of entities, all of which involve the enhancement of unaffected pulmonary vessels coursing through non- or hypo-enhancing consolidated lung parenchyma. Correlation of the imaging findings with the clinical findings may help to further narrow the differential diagnosis to a specific entity<sup>[36]</sup>.

### Adverse drug reaction to gadolinium-containing contrast agents

The overall safety of gadolinium-containing contrast agents has been well established and the frequency of adverse drug reactions with gadolinium-containing contrast agents is lower than with non-ionic iodinated contrast media. It may be beneficial in patients that cannot tolerate intravenous iodinated contrast materials for CT studies; however, recent reports strongly correlated the development of nephrogenic systemic fibrosis with exposure to gadolinium-containing MRI contrast agents (especially, gadodiamide hydrate) in patients with severe renal dysfunction and in post-liver transplantation patients<sup>[37]</sup>. As the United States Food and Drug Administration has issued new information on gadolinium-containing contrast agents<sup>[38]</sup>, radiologists as well as physicians should use these contrast materials with caution because contrast-enhanced MRI has a limited role in the evaluation of SPNs.

### Perspectives and conclusion

Studies evaluated with contrast-enhanced MRI provide a lot of new information. The differentiation between active infections, acute inflammatory lesions, focal organizing pneumonias, well-enhancing benign SPNs (e.g., sclerosing hemangioma and intrapulmonary lymph nodes), and other malignant SPNs, however, requires further evaluation. More case-by-case correlations with histopathology are needed.

For primary lung cancer, bronchial arterial circulation provides the dominant blood supply. In contrast, the pulmonary artery component increases when the location of the tumor is more peripheral<sup>[39,40]</sup> and/or the size is smaller (earlier stage). It is very important to investigate the blood supply of lung cancer. Therefore, the first pass of contrast agents through the intratumoral

microcirculation should be evaluated with dynamic MRI, which has a higher temporal resolution (i.e., acquisition of images every second or several tens of milliseconds), because the pulmonary circulation is 4.0–5.0 s and the pulmonary capillary circulation is 0.7 s in adults<sup>[41]</sup>.

In conclusion, dynamic MRI is useful for differentiating malignant SPNs from benign SPNs (especially tuberculomas and hamartomas). However, it is difficult to differentiate between acute inflammatory lesions and active infection and malignant lesions. Although there are several recent reports on the management and decision trees for SPNs found incidentally<sup>[1–3]</sup>, dynamic MRI might be included as one of the methods for evaluating the enhancing effect of an SPN in addition to dynamic helical CT or FDG-PET if contrast-enhanced CT or FDG-PET is not possible (e.g. allergy to contrast media).

Furthermore, dynamic MRI is useful for assessing tumor vascularity (microvessel density), interstitium (degree of elastic and collagen fibers), and VEGF expression, and for predicting survival outcome among patients with peripheral pulmonary carcinoma. These advantages make dynamic MRI a promising method and a potential biomarker for characterizing tumor response to anti-angiogenic treatment as well as for predicting survival outcomes after treatment.

### Acknowledgments

The work described in this paper was partially supported by a Grant-in-Aid for Scientific Research (C) (grant no. 18591371) from the Japan Society for the Promotion of Science.

### References

- [1] Ost D, Fein AM, Feinsilver SH. The solitary pulmonary nodule. *N Engl J Med* 2003; 348: 2535–42(review).
- [2] Tan BB, Flaherty KR, Kazerooni EA, Iannettoni MD. The solitary pulmonary nodule. *Chest* 2003; 123: 89–96(review).
- [3] Winer-Muram HT. The solitary pulmonary nodule. *Radiology* 2006; 239: 34–49.
- [4] Shaffer K. Role of radiology for imaging and biopsy of solitary pulmonary nodule. *Chest* 1999; 116: 519–522(review).
- [5] MacMahon H, Austin JHM, Gamsu G *et al.* Guidelines for management of small pulmonary nodules detected on CT scans. A statement from the Fleischner Society. *Radiology* 2005; 237: 395–400.
- [6] Erasmus JJ, McAdams HP, Connolly JE. Solitary pulmonary nodules. Part II. Evaluation of the indeterminate nodule. *RadioGraphics* 2000; 20: 59–66.
- [7] Gurney JW. Determining the likelihood of malignancy in solitary pulmonary nodules with Bayesian analysis. Part I. Theory. *Radiology* 1993; 186: 405–13.
- [8] Swensen SJ, Viggiano RW, Midthun DE *et al.* Lung nodule enhancement at CT: multicenter study. *Radiology* 2000; 214: 73–80.
- [9] Yi CA, Lee KS, Kim EA *et al.* Solitary pulmonary nodules: dynamic enhanced multi-detector row CT study and comparison with vascular endothelial growth factor and microvessel density. *Radiology* 2004; 233: 191–9.

- [10] Lee KS, Yi CA, Jeong SY *et al*. Solid or partly solid solitary pulmonary nodules: their characterization using contrast wash-in and morphologic features at helical CT. *Chest* 2007; 131: 1516–25.
- [11] Tomiyama N, Yasuhara Y, Nakajima Y *et al*. CT-guided needle biopsy of lung lesions: a survey of severe complication based on 9783 biopsies in Japan. *Eur J Radiol* 2006; 59: 60–4.
- [12] Gould MK, Maclean CC, Kuschner WG, Ryzak CE, Owens DK. Accuracy of positron emission tomography for diagnosis of pulmonary nodules and mass lesions: a meta-analysis. *JAMA* 2001; 285: 914–24.
- [13] Nomori H, Watanabe K, Ohtsuka T, Naruke T, Suemasu K, Uno K. Evaluation of F-18 fluorodeoxyglucose (FDG) PET scanning for pulmonary nodules less than 3 cm in diameter, with special reference to the CT images. *Lung Cancer* 2004; 45: 19–27.
- [14] Jaruskova M, Belohlavek O. Role of FDG-PET and PET/CT in the diagnosis of prolonged febrile states. *Eur J Nucl Med Mol Imaging* 2006; 33: 913–18.
- [15] Fujimoto K, Edamitsu O, Meno S *et al*. Gd-DTPA-enhanced dynamic magnetic resonance imaging in pulmonary disease: evaluation of usefulness in differentiating benign from malignant disease. *Radiology* 1993; 189(P): 438.
- [16] Fujimoto K, Abe T, Müller NL *et al*. Small peripheral pulmonary carcinomas evaluated with dynamic MR imaging: correlation with tumor vascularity and prognosis. *Radiology* 2003; 227: 786–93.
- [17] Ohno Y, Hatabu H, Takenaka D *et al*. Metastases in mediastinal and hilar lymph nodes in patients with non-small cell lung cancer: quantitative and qualitative assessment with STIR turbo spin-echo MR imaging. *Radiology* 2004; 231: 872–9.
- [18] Schaefer JF, Vollmar J, Schick F *et al*. Solitary pulmonary nodules: dynamic contrast-enhanced MR imaging—perfusion differences in malignant and benign lesions. *Radiology* 2004; 232: 544–53.
- [19] Schaefer JF, Schneider V, Vollmar J *et al*. Solitary pulmonary nodules: association between signal characteristics in dynamic contrast enhanced MRI and tumor angiogenesis. *Lung Cancer* 2006; 53: 39–49.
- [20] Kono R, Fujimoto K, Terasaki H *et al*. Dynamic MRI of solitary pulmonary nodules: comparison of enhancement patterns of malignant and benign small peripheral lung lesions. *AJR Am J Roentgenol* 2007; 188: 26–36.
- [21] Hylton N. Dynamic contrast-enhanced magnetic resonance imaging as an imaging biomarker. *J Clin Oncol* 2006; 24: 3293–8.
- [22] Yi CA, Jeon TY, Lee KS *et al*. 3-T MRI: usefulness for evaluating primary lung cancer and small nodules in lobes not containing primary tumors. *AJR Am J Roentgenol* 2007; 186: 386–92.
- [23] Heelan RT, Demas BE, Caravelli JF *et al*. Superior sulcus tumors: CT and MR imaging. *Radiology* 1989; 170: 637–41.
- [24] Webb WR, Gatsonis C, Zerhouni EA *et al*. CT and MR imaging in staging non-small cell bronchogenic carcinoma: report of the Radiologic Diagnostic Oncology Group. *Radiology* 1991; 178: 705–13.
- [25] Ohno Y, Hatabu H, Takenaka D *et al*. Metastases in mediastinal and hilar lymph nodes in patients with non-small cell lung cancer: quantitative and qualitative assessment with STIR turbo spin-echo MR imaging. *Radiology* 2004; 231: 872–9.
- [26] Jeswani T, Padhani AR. Imaging tumour angiogenesis. *Cancer Imaging* 2005; 5: 131–8.
- [27] Parker GJ, Suckling J, Tanner SF *et al*. Probing tumor microvascularity by measurement, analysis and display of contrast agent uptake kinetics. *J Magn Reson Imaging* 1997; 7: 564–74.
- [28] Cheung N, Wong MP, Yuen ST, Leung SY, Chung LP. Tissue-specific expression pattern of vascular endothelial growth factor isoforms in the malignant transformation of lung and colon. *Hum Pathol* 1998; 29: 910–14.
- [29] Tateishi U. Vascular endothelial growth factor—related angiogenesis. *Radiology* 2005; 235: 1084–5.
- [30] Libby DM, Wu N, Lee IJ *et al*. CT screening for lung cancer: the value of short-term CT follow-up. *Chest* 2006; 129: 1039–42.
- [31] Sakai F, Sone S, Maruyama A *et al*. Thin-rim enhancement in Gd-DTPA-enhanced magnetic resonance imaging of tuberculoma: a new finding of potential differential diagnosis importance. *J Thorac Imaging* 1992; 7: 64–9.
- [32] Murayama S, Murakami J, Hashimoto S *et al*. Noncalcified pulmonary tuberculosis. CT enhancement pattern with histological correlation. *J Thorac Imaging* 1995; 10: 91–5.
- [33] Fujimoto K, Müller NL, Sadohara J *et al*. Alveolar adenoma of the lung: computed tomography and magnetic resonance imaging findings. *J Thorac Imaging* 2002; 17: 163–6.
- [34] Sakai F, Sone S, Kiyono K *et al*. MR of pulmonary hamartoma. pathologic correlation. *J Thorac Imaging* 1994; 9: 51–5.
- [35] Im JG, Han MC, Yu EJ *et al*. Lobar bronchioloalveolar cell carcinoma: angiogram sign on CT scans. *Radiology* 1990; 176: 749–53.
- [36] Maldonado RL. The CT angiogram sign. *Radiology* 1999; 210: 323–4.
- [37] Public Health Advisory. Gadolinium-containing contrast agents for magnetic resonance imaging (MRI): Omniscan, OptiMARK, Magnevist, ProHance, and MultiHance. [http://www.fda.gov/cder/drug/advisory/gadolinium\\_agents.htm](http://www.fda.gov/cder/drug/advisory/gadolinium_agents.htm)
- [38] Information on gadolinium-containing contrast agents. <http://www.fda.gov/cder/drug/infopage/gcca/default.htm>
- [39] Milne EN. Circulation of primary and metastatic pulmonary neoplasms. A postmortem microarteriographic study. *Am J Roentgenol Radium Ther Nucl Med* 1967; 100: 603–19.
- [40] Ohno Y, Hatabu H, Takenaka D *et al*. Dynamic MR imaging: value of differentiating subtypes of peripheral small adenocarcinoma of the lung. *Eur J Radiol* 2004; 52: 144–50.
- [41] Levitzky MG. Blood flow to the lung. In: *Pulmonary physiology*. 5th ed. New York: McGraw-Hill; 1999, p. 85–111.